

# ON THE USE OF THE M-QUANTILES FOR OUTLIER DETECTION IN MULTIVARIATE DATA

BY SAJAL CHAKROBORTY<sup>a</sup> AND RAM IYER<sup>b</sup>  AND A. ALEXANDRE TRINDADE<sup>c</sup>

*Department of Mathematics and Statistics, Texas Tech University, USA*, <sup>a</sup>[sajal.chakroborty@ttu.edu](mailto:sajal.chakroborty@ttu.edu); <sup>b</sup>[ram.iyer@ttu.edu](mailto:ram.iyer@ttu.edu); <sup>c</sup>[alex.trindade@ttu.edu](mailto:alex.trindade@ttu.edu)

Defining a successful notion of a multivariate quantile has been an open problem for more than half a century, motivating a plethora of possible solutions. Of these, the approach of [8] and [25] leading to M-quantiles, is very appealing for its mathematical elegance – combining elements of convex analysis and probability theory. The key idea is the description of a convex function (the K-function) whose gradient (the K-transform) is in one-to-one correspondence between all of  $\mathbb{R}^d$  and the unit ball in  $\mathbb{R}^d$ . By analogy with the  $d = 1$  case where the K-transform is a cumulative distribution function-like object (an M-distribution), the fact that its inverse is guaranteed to exist lends itself naturally to providing the basis for the definition of a quantile function for all  $d \geq 1$ . Over the past twenty years the resulting M-quantiles have seen applications in a variety of fields, primarily for the purpose of detecting outliers in multidimensional spaces. In this article we prove that for odd  $d \geq 3$ , it is not the gradient but a poly-Laplacian of the K-function that is (almost everywhere) proportional to the density function. For  $d$  even one cannot establish a differential equation connecting the K-function with the density. These results show that usage of the K-transform for outlier detection in higher odd-dimensions is in principle flawed, as the K-transform does not originate from inversion of a true M-distribution. We demonstrate these conclusions in two dimensions through examples from non-standard asymmetric distributions. Our examples illustrate a feature of the K-transform whereby regions in the domain with higher density map to larger volumes in the co-domain, thereby producing a magnification effect that moves inliers closer to the boundary of the co-domain than outliers. This feature obviously disrupts any outlier detection mechanism that relies on the inverse K-transform.

## CONTENTS

1	Introduction . . . . .	2
2	The K-transform: Definition and Outlier Detection . . . . .	5
3	The K-transform in Relation to the Distribution . . . . .	7
4	The zoom-in effect for $\mathbb{R}^2$ . . . . .	9
5	Conclusion . . . . .	11
A	Algorithm for Computation of Geometric Quantiles . . . . .	11
B	Proof of Theorem 2.1 . . . . .	12
C	Proof of Lemma 3.2 . . . . .	13
D	Proof of Lemma 3.3 . . . . .	14
E	Proof of Lemma 3.4 . . . . .	15
F	Proof of Lemma 3.5 . . . . .	17
G	Proof of Theorem 3.6 . . . . .	18
H	Proof of Corollary 1 . . . . .	19
	References . . . . .	19

---

*Keywords and phrases:* multivariate distribution function, multivariate quantile, geometric quantile, outlier detection.

**1. Introduction.** The subject of outlier detection has a long history in the statistical and data-mining literature. This harks at the difficulty of the enterprise, which reflects the fact that a precise definition is elusive. Thus, while there is general agreement that an outlier is an observation that deviates so much from the others as to arouse suspicion, or appears to be inconsistent with the remainder of the data, there is much debate on how to measure the actual “deviation” or “inconsistency” [3].

For univariate data that can plausibly be modeled as a realization of a random sample (independent and identically distributed, or i.i.d.), most detection methods rely on the quantile function of the data generating mechanism. In the taxonomy of the field one can distinguish between parametric methods which classify outliers as those lying on the tails of the distribution, and nonparametric methods that rely on inter-quantile ranges [47]. For multivariate data, the inherent difficulty in defining quantiles in multidimensional spaces has shifted the focus to measuring the distance of individual points from the center of the data cloud. Thus one finds a substantial body of literature on such *distance functions*, or their inverses, *depth functions*; see for example [34] for a survey, and [49] for formal definitions and theoretical development.

Quantiles are calculated by inverting the cumulative distribution function (cdf). Mathematically, for any random variable  $X$  defined on  $\mathbb{R}$ , the most generally accepted definition of the quantile function at probability level  $s$ , is the mapping  $Q : [0, 1] \mapsto \mathbb{R}$ , given by

$$(1) \quad Q(s) = \inf\{x : F(x) \geq s\},$$

where  $F(x) = P(X \leq x)$  denotes the cdf of  $X$ , corresponding to a left-to-right accumulation of mass. In one dimension, the only other essentially different mass accumulation would be center-outward (with “center” taken to be, e.g., the median). We term  $\bar{F}(x) = 2F(x) - 1$  the *signed* cdf. It is the so-called *M-distribution* arrived at by [25] when attempting to extend the notion of a quantile. [28] notes that goodness-of-fit tests like Kolmogorov-Smirnov based on mass accumulation dictated by  $|\bar{F}(x)|$ , which corresponds to a center-outward ordering, are more powerful at detecting scale differences. Such a center-outward ordering also features prominently in [23], who define a multivariate cdf (and associated quantile function) based on the intriguing concept of transportation-based ranks and signs. One may therefore define an alternate quantile function based on the mapping  $\bar{Q} : [-1, 1] \mapsto \mathbb{R}$ , given by

$$(2) \quad \bar{Q}(s) = \inf\{x : \bar{F}(x) \geq s\}.$$

As there is no natural ordering in multidimensional spaces (dimension  $d$  in general), it is difficult to extend the notion of a quantile. Early contributions to this field of study were made by [22], [5], [36], [4], and [11], among others. [42] provides a comprehensive overview and an exhaustive comparison of the different methodologies. Although it is not our intent to give an updated survey here, we highlight two approaches that serve to give some idea of the difficulties involved. [4] define an M-quantile through the notion of an M-estimator and its associated loss and influence functions. Although this leads to sensible definitions for the median, e.g., under radially symmetric loss we obtain the geometric median (discussed in detail below), the quantile extension is cumbersome and suffers from a high computational burden. Another definition for finite as well as for infinite-dimensional spaces (e.g., functional data) was proposed by [18]. Their approach however, which builds on earlier ideas by [26] and others that rely on directional projections of the probability measure onto the unit sphere, leads to quantiles that are not affinely equivariant. (Instead of plotting quantile contours, they proposed computing principal quantile directions in order to detect outliers.)

A common thread in these various attempts to generalize the notion of a quantile, is the imposition of the requirement that the specialization to the univariate case corresponds to the quantile function  $Q$  or  $\bar{Q}$ . Any such attempt must also by necessity be grounded on the

simpler problem of leading to the special case of a well-defined median. In this regard, it has long been noted that  $Q(0.5)$  minimizes the mean absolute error ([45]),

$$Q(0.5) = \arg \min_{c \in \mathbb{R}} \mathbb{E}|X - c| = \arg \min_{c \in \mathbb{R}} \mathbb{E}(|X - c| - |X|),$$

where the last expression is to be used in cases when the expectation does not exist. By extension, the minimizer of the multivariate mean absolute error is typically defined as the multivariate median:

$$(3) \quad \text{Med}_p = \arg \min_{s \in \mathbb{R}^d} \mathbb{E}(\|X - s\|_p - \|X\|_p),$$

where  $\|\cdot\|_p$  denotes the  $L^p$ -norm in  $\mathbb{R}^d$ . In the literature, one finds both the  $L^2$ -norm (Euclidean distance) and  $L^1$ -norm (Manhattan distance) used in (3); [37] calls the former the *spatial median*, and the latter the *marginal median* (vector of marginal medians). The marginal median, first studied by [38] and later investigated for outlier detection in [7], suffers from lack of invariance with respect to coordinate rotations, or more precisely, actions of the special orthogonal group  $SO(d)$ . Other names in common usage when the 2-norm is employed in (3), include *geometric median* and  *$L^1$  median* ([44, 30, 39]). It is easily shown that geometric median is invariant with respect to coordinate rotations and translations of the origin. Henceforth in this article, we will consider the  $L^2$ -norm in Equation (3) as we attempt to generalize and clarify various notions.

Chaudhuri [12] extended the notion of the geometric median and defined a quantity that he referred to as the *geometric quantile*. For  $v \in B_1(0)$ , the open unit ball in  $\mathbb{R}^d$ , this is given by

$$(4) \quad Q_G(v) = \arg \min_{s \in \mathbb{R}^d} \mathbb{E}\{\|X - s\|_2 + \langle v, X - s \rangle - \|X\|_2 - \langle v, X \rangle\},$$

where  $\langle \cdot, \cdot \rangle$  denotes the usual Euclidean inner product. The justification given for referring to this as a *quantile* is that  $Q_G(0)$  corresponds to the geometric median, i.e., (3) with  $p = 2$ . Contemporaneously, Koltchinskii [25] developed a function (henceforth *K-function*), which in principle resembles the integral of a multivariate cdf,

$$(5) \quad f(s) = \mathbb{E}[\|s - X\|_2 - \|X\|_2].$$

If we now consider the subdifferential function  $\partial f(s)$ , which we call the *K-transform* (defined in (9) with explicit reference to the underlying measure  $\mu$ ), Koltchinskii's *M-quantile* is then the inverse K-transform, which constitutes his attempt at defining a multivariate quantile. To relate Chaudhuri's notion of a quantile to Koltchinskii's, note that:

$$(6) \quad Q_G(v) = \arg \min_{s \in \mathbb{R}^d} \mathbb{E}\{\|X - s\|_2 + \langle v, X - s \rangle\} = \arg \max_{s \in \mathbb{R}^d} \mathbb{E}\{\langle v, s - X \rangle - \|s - X\|_2\}.$$

Now, since  $f(s)$  is convex in  $s$ , we see that the function  $Q_G(v)$  is simply the Fenchel conjugate of  $f(s)$ .

The noteworthy difference between these two approaches is that, whereas [12] directly defines  $Q_G(v)$  as a quantile without relating it to the inverse of a suitably defined cdf, [25] starts with  $f(s)$ , defines  $\partial f(s)$  as an *M-distribution* (which coincides with the signed cdf  $\bar{F}(s)$  in the unidimensional case), and uses results from convex analysis to obtain  $Q_G(v) = \partial f^{-1}(v)$ . An immediate corollary of this fact is that the geometric quantile uniquely determines the underlying distribution ([25]). [7] claims that this property may be used for outlier detection, in that values of  $\|Q_G(v)\|_2$  closer to one are indicative of outliers. However, [13] notes that this claim may not hold in  $\mathbb{R}^2$ , by demonstrating that outliers may have a smaller value of  $\|Q_G(v)\|$  than inliers for non-standard distributions such as mixtures of Gaussians. However,

$d = 2$  is a special case for the K-transform as may be seen in [7, Theorem 3.2], and it is unclear whether outlier detection may be performed for higher dimensional data.

The concept of geometric quantiles has been a very active area of research. Although it is not very useful for outlier detection beyond two dimensions as we show in this article, it is aesthetically pleasing due to connections with convex analysis. The mathematical elegance also permits generalizations to infinite dimensional Banach spaces. With equation (4) as the population geometric quantile, the empirical geometric quantile for a  $d$ -dimensional sample of  $n$  data points  $\{x_1, \dots, x_n\}$  is

$$(7) \quad \widehat{Q}_G(v) = \arg \min_{s \in \mathbb{R}^d} \frac{1}{n} \sum_{i=1}^n \{ \|x_i - s\|_2 + \langle v, x_i - s \rangle - \|x_i\|_2 - \langle v, x_i \rangle \}.$$

[12] and [7] have derived a Bahadur-type representation for  $\widehat{Q}_G(v)$ , and proved Glivenko-Cantelli and Donsker-type results. [6] have extended these results for data on infinite dimensional Banach spaces. Although the quantiles in (4) are equivariant under rotations of the data cloud, they are not equivariant under affine transformations. [8] develop the notion of an affine equivariant multivariate median for finite dimensional data, and [7] extend this notion to  $L^p$  spaces. Computation of  $Q_G(v)$  has however been a stumbling block beyond the simplest of distributions. In Appendix A we present an algorithm for this purpose.

Several extensions and applications of these M-quantiles have appeared in the literature. Their main use has been to effect outlier detection in areas as varied as manufacturing processes, image processing, economic models, risk assessment, and biostatistics. With very few exceptions, these are all closely related to the geometric quantiles of [12] or the inverse K-transform of [25] (which are essentially identical as explained earlier). They were proposed as a means to detect outliers in two-dimensional data in [7] and [10]. However, the underlying distributions were only chosen to be the Gaussian, and hence this paradigm may not generalize well. It has also been proposed that regions of low probability density should be associated with outliers in data ([9, 1]).

Various tools called projection quantiles ([35]), quantile contour plots ([7, 10, 20]), multivariate quantile-quantile (QQ) plots ([7, 31, 16]), and spatial depth functions ([43]), have been developed based on these M-quantiles. Some applications of these tools include [13] who use them for outlier detection in images, [15] for image denoising through spatial depth, and [46] who devised a calibration methodology to improve the quality of the electrocardiograms. The concept of M-quantiles has also found uses in risk assessment ([24]), control charts in manufacturing processes ([29]), climate modeling ([17]), and development of economic models ([2]).

In this article, we will investigate the connection between the probability density function (pdf) and the K-function in order to determine the utility of the K-transform for outlier detection in multivariate data. For  $d = 1$ , note that the K-transform  $\nabla f(s) = f'(x) = \overline{F}(x)$ , which reduces to the signed cdf. (This was the original motivation of [25] in defining  $\partial f(s)$  as an M-distribution.) Thus  $f''(s) = 2\rho(s)$  almost everywhere, where  $\rho(\cdot)$  is the underlying pdf of  $X$ . As we will show, this is the only case where differentials of the K-transform lead directly to the pdf. Specifically, and with regard to continuous measures only for which the subdifferential reduces to the ordinary differential (or gradient),  $\partial f(s) = \nabla f(s)$ , this article makes the following contributions.

- For odd dimensions  $d \geq 3$ , we show it is in fact the poly-Laplacian of order  $(d + 1)/2$  of  $f(s)$  that is (almost everywhere) equal to a scalar multiple of  $\rho(s)$ . If one is to believe that regions of low probability density are indicative of outliers and anomalies in data (e.g., [9, 1]), then this shows that  $\nabla f(s)$  does not directly lead to the discovery of regions of low or high probability density in high odd dimensional spaces. Thus the M-distribution of [25] cannot be considered as a distribution in any sense in higher dimensional spaces.

- For dimension  $d = 2$  we elucidate the reason for the observation of [13] mentioned above, that values of  $\|Q_G(v)\|_2 \approx 1$  are not necessarily indicative of outliers. It was shown by [25] that the K-transform is in a one-to-one correspondence between  $\mathbb{R}^d$  and the open unit ball in  $\mathbb{R}^d$ . However, as we will show, the K-transform has a zoom-in effect whereby regions of high density occupy a higher volume in the co-domain, and conversely, regions of low density occupy a smaller volume. Due to this effect, the distance of a point from the origin in the co-domain does not necessarily imply that the point lies in a low density region of the distribution (as would an outlier).
- Exploiting the connections with convexity theory, we propose an algorithm to compute the geometric quantile  $Q_G(v)$ . The algorithm, based on the MM principle [27], allows one to easily verify the numerical results obtained by [7] and [13], and to compute the inverse of the K-transform, even for highly nonstandard distributions, and in any finite dimensional vector space.

These results lead to the main conclusion of this article: that the K-transform cannot theoretically be considered to be a distribution for dimensions  $d \geq 2$ , and consequently, that its inverse cannot be viewed as a quantile function. The remainder of the paper is structured as follows. The K-transform and its inverse are defined and discussed in Section 2. In Section 3, we present formal results of the points made above concerning the K-transform and empirical geometric quantile, and discuss their significance. In Section 4, we present numerical examples to illustrate the zoom-in effect of the K-transform, and comment on its potential use for outlier detection in two dimensional data. The proofs of all formal results are relegated to the appendix.

Before we proceed to the formal definitions, we note that a related approach of using a convex function to define center-outward distribution and quantiles has seen attention in the literature lately [14, 23, 19]. This approach uses the celebrated Brenier-McCann theorem that asserts the existence of a convex function whose gradient transports a reference distribution absolutely continuous with respect to the Lebesgue measure on  $\mathbb{R}^d$  to the population distribution [32]. The convex function from this method does not have a formula and therefore cannot be directly analyzed as we have done for the K-function. However, we note that the center-outward quantile contours are proved to be *connected*, closed, nested, with continuous boundaries [23]. We foresee that the connectedness of the quantile contour would cause difficulties in detecting outliers for the non-standard distributions from [48] depicted in Figure 3(a) and 4(a) respectively, but we do not investigate this method any further in this article.

**2. The K-transform: Definition and Outlier Detection.** Let  $(\mathbb{R}^d, \mathcal{F}, \mu)$  be a probability space. For any  $s \in \mathbb{R}^d$ , the Koltchinskii function (K-function) is defined as the integral transform of  $f(s, x) = \|s - x\|_2 - \|x\|_2$  with respect to  $\mu$ :

$$(8) \quad f_\mu(s) = \mathbb{E}f(s, x) = \int_{\mathbb{R}^d} (\|x - s\|_2 - \|x\|_2) \mu(dx).$$

It is easily verified that  $f_\mu$  is a convex function. The K-transform ([25]), is defined in as the sub-differential of  $f_\mu$ . For  $s \in \mathbb{R}^d$ ,

$$(9) \quad \partial f_\mu(s) = \int_{\mathbb{R}^d} \frac{s - x}{\|s - x\|_2} \mu(dx).$$

The K-transform is in one-to-one correspondence between  $\mathbb{R}^d$  and the open unit ball  $B_1(0)$ . Now consider the conjugate function of  $f_\mu$ , given by,

$$(10) \quad f_\mu^*(v) = \sup_{s \in \mathbb{R}^d} [\langle s, v \rangle - f_\mu(s)], \quad v \in B_1(0).$$

The subdifferential of  $f_\mu^*$  exists ([40]), and is given by  $\partial f_\mu^* = (\partial f_\mu)^{-1}$ . The map  $\partial f_\mu^*$  is the inverse K-transform, and is referred to as an M-quantile ([25]). For dimension  $d = 1$ , the K-transform is the signed cdf  $\partial f_\mu(s) = \mu((-\infty, s]) - \mu([s, \infty)) := \bar{F}(s)$ . In this case, the inverse K-transform is interpreted as a quantile function. Also for  $d = 1$ , there are well-established techniques for outlier detection in data based on quantile plots, due to the facts that there is a natural ordering on the real line, and the derivative of the K-transform is the density.

The inverse K-transform has been proposed as a means to detect outliers in two-dimensional data (see e.g., [7] and [10]). However, the underlying distributions were chosen to be the Gaussian, which is one of the simplest of cases. Figure 1 illustrates the potentially misleading result obtained in [7]. In Figure 1(a), we have plotted 3000 data points from a bivariate normal distribution with zero mean, unit standard deviation, and a correlation coefficient of 0.75. The contours here are the inverse K-transform of the contours in Figure 1(b). [7] proposes that data points falling outside the inverse K-transform pertaining to contours of the K-transform with a large radius (say  $r \geq 0.9$ ) may be classified as outliers. In Section 4 we present numerical simulations with more complex densities that reveals a very interesting feature of the K-transform that we call the *zoom-in* effect. Due to this effect, we cannot interpret the radial distance from the origin in Figure 1(a) as representing “quantiles”, a view that could lead to potentially erroneous outlier detection results.

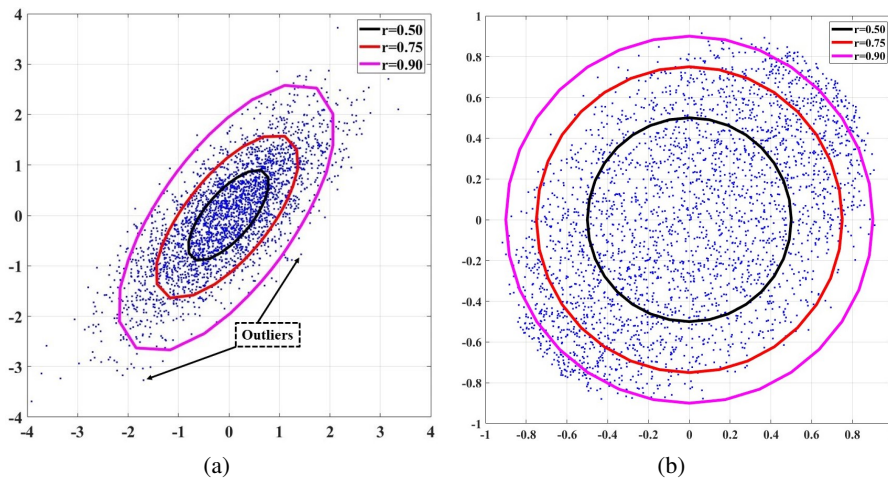


FIG 1. K-transform and its inverse for a bivariate Gaussian with zero mean, unit standard deviation, and correlation coefficient of 0.75. The K-transform is shown in Figure 1(b), and the inverse K-transform in Figure 1(a), along with 3000 data points simulated from the distribution.

Our main result in the next section will show that for odd  $d \geq 3$ , a poly-Laplacian of the K-function is proportional to the pdf. The proof of this result requires the following non-trivial measure theoretic version of the Leibniz Rule. We state this here as a major result in its own right.

**THEOREM 2.1 (Lebesgue Measure Leibniz Rule).** *Suppose  $f(s, x)$  is bounded for all  $x \in [a, b]$ , and is both bounded and integrable with respect to Lebesgue measure  $\lambda$  for all  $s \in [\alpha, \beta]$ . For any Lipschitz continuous functions  $g, h : [\alpha, \beta] \rightarrow [a, b]$ , let:*

$$\phi(s) = \int_{h(s)}^{g(s)} f(s, x) dx.$$

For all  $s \in (\alpha, \beta)$  and for all  $x \in [a, b] \setminus E_0$ , where  $\lambda(E_0) = 0$ , let  $\partial f(s, x)/\partial s$  be defined on  $(\alpha, \beta) \times [a, b]$  and bounded in absolute value. Then, for almost all  $s \in (\alpha, \beta)$ , the derivative  $d\phi(s)/ds$  exists and can be split as follows:

$$(11) \quad \frac{d}{ds}\phi(s) = f(s, g(s)) \frac{dg(s)}{ds} - f(s, h(s)) \frac{dh(s)}{ds} + \int_{[h(s), g(s)] \setminus E_0} \frac{\partial}{\partial s} f(s, x) dx.$$

**3. The K-transform in Relation to the Distribution.** In this section, we will present our main result concerning the relationship of the K-transform to the distribution of the underlying random vector  $X$  in a probability space  $(\mathbb{R}^d, \mathcal{F}, \mu)$ . We will show that for any odd values of the dimension  $d$ , it is in fact the poly-Laplacian of the K-function that corresponds to a scalar multiple of the pdf  $\rho(x)$  of  $X$ .

Let  $s \in \mathbb{R}^d$  be a given point. Let  $\sigma_k$  denote the hypersurface area measure on the  $k$ -sphere. For example, when  $d = 2$  we have

$$d\sigma_1(\varphi_1) = d\varphi_1, d\sigma_2(\varphi_1, \varphi_2) = \sin(\varphi_2) d\varphi_1 d\varphi_2,$$

and in general,

$$d\sigma_k(\varphi_1, \varphi_2, \dots, \varphi_k) = \prod_{j=1}^k \sin^{j-1}(\varphi_j) d\varphi_j, \quad k = 1, 2, 3, \dots$$

For simplicity, write  $\Phi_k$  for the angular tuple  $(\varphi_1, \varphi_2, \dots, \varphi_k)$ . The volume element of  $x \in \mathbb{R}^d$  represented by the polar coordinates  $(r, \varphi_1, \varphi_2, \dots, \varphi_{d-1})$ , where  $r$  is the distance of  $x$  from  $s$ , is given by

$$dV(x) = r^{d-1} dr d\sigma_{d-1}(\Phi_{d-1}).$$

An essentially bounded function  $\rho: \mathbb{R}^d \rightarrow \mathbb{R}_+$ , satisfying

$$\int_{\mathbb{R}^d} \rho(x) dV(x) = 1,$$

is said to be a *bounded density* (bounded pdf). On the sigma-algebra of Borel subsets of  $\mathbb{R}^d$ , we may use  $\rho$  to define a Radon measure as arising from a positive linear form on  $C_c(\mathbb{R}^d)$ , the set of continuous functions with compact support on  $\mathbb{R}^d$ . Alternatively, one starts with an absolutely continuous Radon measure with respect to the Lebesgue measure, and takes its Radon-Nikodym derivative to be the density  $\rho$ .

**REMARK 3.1.** Note that if  $\mu(dx) = \rho(x)dV(x)$ , then the K-transform is simply the gradient of the K-function, so that  $\partial f_\mu(s) = \nabla f_\mu(s)$  in (9).

The lemma below is a building block on which the theory is based. It shows that the expectation of certain singular kernels is in fact well defined. The only mild requirement is that the probability density should be bounded.

**LEMMA 3.2.** Suppose  $\rho(x)$  is a bounded pdf for the random vector  $X$  on  $\mathbb{R}^d$ , with  $d \geq 3$ . Then, for any  $s \in \mathbb{R}^d$ , the function defined as

$$(12) \quad G(s) = \int_{\mathbb{R}^d} \|s - x\|_2^{-k} \rho(x) dV(x),$$

exists for any  $k = 0, \dots, d - 1$ .

The second lemma shows that the gradient of  $G(s)$  defined above exists for  $0 \leq k \leq d - 2$ .

LEMMA 3.3. *Suppose  $\rho(x)$  is a bounded pdf on  $\mathbb{R}^d$ , for  $d \geq 3$ . Then, for any  $s \in \mathbb{R}^d$  and  $k = 0, \dots, d - 2$ , the Frechet derivative of  $G(s)$  defined in (12) with respect to  $s$ , exists and is given by*

$$(13) \quad \nabla_s G(s) = -k \int_{\mathbb{R}^d} \frac{(s-x)}{\|s-x\|_2^{k+2}} \rho(x) dV(x).$$

The third lemma shows that the Hessian of  $G(s)$  exists for  $0 \leq k \leq d - 3$ . The Hessian computation is important as the Laplacian may be computed as the trace of the Hessian matrix.

LEMMA 3.4. *Suppose  $\rho(x)$  is a bounded pdf on  $\mathbb{R}^d$  for  $d \geq 3$ . Then, for any  $s \in \mathbb{R}^d$  and  $k = 0, \dots, d - 3$ , the Hessian of  $G(s)$  defined in (12) with respect to  $s$ , is given by:*

$$(14) \quad D_s G(s) = -k \int_{\mathbb{R}^d} \left( \frac{I_d}{\|s-x\|_2^{k+2}} - (k+2) \frac{(s-x)(s-x)^t}{\|s-x\|_2^{k+4}} \right) \rho(x) dV(x).$$

We are now ready to produce results for the K-transform. The lemma below considers the univariate case ( $d = 1$ ); the special case of odd dimension that is omitted in the statement of Theorem 3.6. The result is proved in [25] using convex analysis. Here we use real analysis techniques, because for dimensions greater than one, they allow one to obtain expressions for the poly-Laplacian of the K-function.

LEMMA 3.5. *Consider the probability space  $(\mathbb{R}, \mathcal{F}, \mu)$ , where the measure  $\mu$  of the random element  $X$  has a bounded density,  $\rho(x)$ , on  $\mathbb{R}$ . Consider the  $d = 1$  version of the K-function defined in (8):*

$$f_\mu(s) = \int_{\mathbb{R}} (|s-x| - |x|) \rho(x) dx.$$

*Then, for almost every  $s \in \mathbb{R}$ , the second derivative of  $f_\mu(s)$  exists, and is given by,*

$$(15) \quad f_\mu''(s) = 2\rho(s).$$

With the above lemmas in place, we can now state the main theoretical result of this article. Taken together, we show that for odd dimensions  $d \geq 3$ , the poly-Laplacian of order  $(d+1)/2$  of the K-function is equal to a scalar multiple of the density (almost everywhere), with the scalar depending only on  $d$ . As regions of low probability density are commonly associated with outliers and anomalies in data (see [9, 1]), this result shows that, contrary to emerging belief, it is not the K-transform  $\nabla f_\mu(s)$  that is directly related to the density, but the poly-Laplacian  $\Delta^{(d+1)/2} f_\mu(s)$  instead. Hence, it is dubious to use the K-transform to compute ‘‘quantiles’’ in odd dimensions  $d \geq 3$ ; a situation that is completely different from the  $d = 1$  case.

Using Lemma 3.4, we can obtain a different type of result for even dimensions. However, we can only establish a lower bound for  $\|\nabla f_\mu(s)\|_2$  for  $d = 2$ , and an upper bound for  $\|\nabla \Delta^{(d-2)/2} f_\mu(s)\|_2$  for  $d \geq 4$ , in terms of  $\rho(s)$ . Unfortunately these results do not appear to have as clear an interpretation as those for odd dimensions.

**THEOREM 3.6.** Consider the probability space  $(\mathbb{R}^d, \mathcal{F}, \mu)$ , where the probability measure  $\mu$  has a bounded density  $\rho(x)$  in  $\mathbb{R}^d$ , and whose K-function  $f_\mu(s)$  is as defined in (8). Let  $\Delta^j f_\mu(s)$  be the poly-Laplacian of order  $j$  of  $f_\mu(s)$ , defined as:

$$(16) \quad \Delta^j f_\mu(s) = (-1)^{j+1} (d-1)(d-3)\dots(d-2j+1) \mathbb{E} \left( \frac{1}{\|s-X\|_2^{2j-1}} \right).$$

Then, for any  $s \in \mathbb{R}^d$  and odd values of the dimension  $d \geq 3$ ,  $\Delta^j f_\mu(s)$  exists for all  $j = 1, \dots, N$ , where  $N = (d-1)/2$ .

**COROLLARY 1.** For any odd  $d \geq 3$ , and for almost every  $s \in \mathbb{R}^d$ , we have that:

$$(17) \quad \Delta^{N+1} f_\mu(s) = \alpha \rho(s),$$

where  $\alpha = (-1)^{N-1} (d-1) \dots (2) d (d-2) \pi^{d/2} / \Gamma(\frac{d}{2} + 1)$ , and  $\Gamma$  is the gamma function.

Note that the first few poly-Laplacians are (assuming odd  $d > 5$ ):

$$\Delta_s f_\mu(s) = (d-1) \mathbb{E} \left( \frac{1}{\|s-X\|_2} \right), \quad \Delta_s^2 f_\mu(s) = (-1)(d-1)(d-3) \mathbb{E} \left( \frac{1}{\|s-X\|_2^3} \right),$$

and

$$\Delta_s^3 f_\mu(s) = (-1)^2 (d-1)(d-3)(d-5) \mathbb{E} \left( \frac{1}{\|s-X\|_2^5} \right).$$

The final polyharmonic is:

$$(18) \quad \Delta_s^N f_\mu(s) = (-1)^{N-1} (d-1) \dots (2) \mathbb{E} \left( \frac{1}{\|s-X\|_2^{d-2}} \right).$$

**4. The zoom-in effect for  $\mathbb{R}^2$ .** The inverse K-transform is useful for detecting outliers in simple distributions on  $\mathbb{R}^2$ , for instance the Gaussian, as demonstrated by [7]. However, [13] cautioned that this claim is incorrect for non-standard distributions in  $\mathbb{R}^2$  such as a mixture of Gaussians. In this section, we demonstrate why this happens by highlighting a special feature of the K-transform that we call the “zoom-in” effect.

Consider the unit disk in  $\mathbb{R}^2$  centered at the origin with a uniform density of  $\pi^{-1}$ . By symmetry of the disk, the K-transform at the point  $s = (s_1, s_2)$  is given by:

$$(19) \quad \nabla f_\mu(s_1, s_2) = \int_{B_1(0)} \frac{(s_1, s_2) - (x_1, x_2)}{\|(s_1, s_2) - (x_1, x_2)\|_2} \mu(dx).$$

As discussed in Section 2, the K-transform will map all of  $\mathbb{R}^2$  onto the unit disk in the codomain. Figures 2, 3, and 4 depict the zoom-in effect on the banana-shaped [23], spiral-shaped [21, 48], and square-shaped [21, 48] distributions. Note that the *zoom-in* effect refers to the tendency of the K-transform to magnify regions of the support, so that they occupy a disproportionately larger area of the unit disk.

The banana-shaped distribution is a mixture of three Gaussian distributions with  $n = 20,000$  sample points, given by,

$$\frac{3}{8} N(-3\tau_1, \Sigma_1) + \frac{3}{8} N(3\tau_1, \Sigma_2) + \frac{1}{4} N(-\frac{5}{2}\tau_2, \Sigma_3),$$

where  $\tau_1 = \begin{pmatrix} 1 \\ 0 \end{pmatrix}$ ,  $\tau_2 = \begin{pmatrix} 0 \\ 1 \end{pmatrix}$ ,  $\Sigma_1 = \begin{pmatrix} 5 & -4 \\ -4 & 5 \end{pmatrix}$ ,  $\Sigma_2 = \begin{pmatrix} 5 & 4 \\ 4 & 5 \end{pmatrix}$ , and,  $\Sigma_3 = \begin{pmatrix} 4 & 0 \\ 0 & 1 \end{pmatrix}$ . The contour lines in Figure 2(a), 3(a), and 4(a) are the inverse K-transform of the contours with radial

distances of 0.5 (blue), 0.75 (red), and 0.90 (maroon) in the codomain. We have used our developed MM-type algorithm to compute the inverse K-transform of the contours that are in the codomain. [7, 20] described the inverse K-contour lines as quantile contours and [7] classified points that are outside of radial distance 0.9 as outliers. From these figures, we can observe that because of the zoom-in effect, inlier points become close to the boundary of the contour lines with a radial distance of 0.9, and outlier points get close to the inliers.

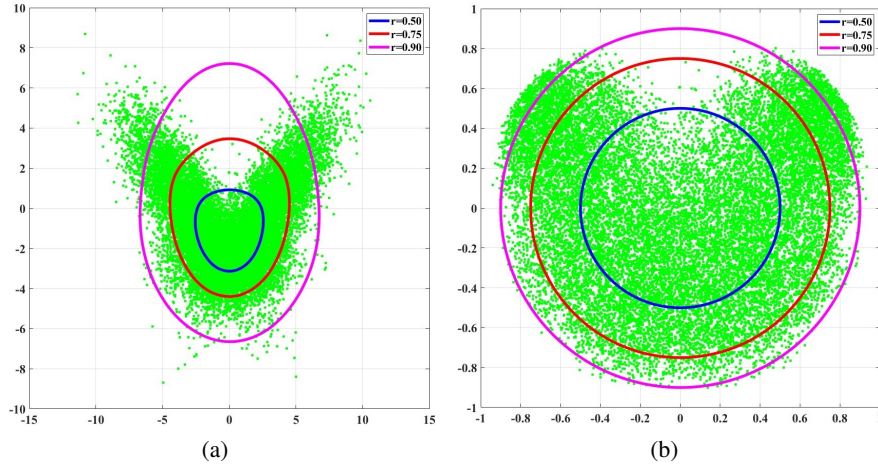


FIG 2. Banana-shaped distribution with  $n = 20,000$  sample points [23]. Concentric circles of radius 0.50 (blue), 0.75 (red), and 0.90 (maroon) are shown in Figure 2(a). Their corresponding K-transforms are in Figure 2(b). This example illustrates the zoom-in effect of the K-transform. Points outside the support of the distribution in the domain occupy a small region close to the boundary of the unit circle in the co-domain. Hence,  $1 - \|\nabla f\|_2$  cannot be interpreted as a depth function.

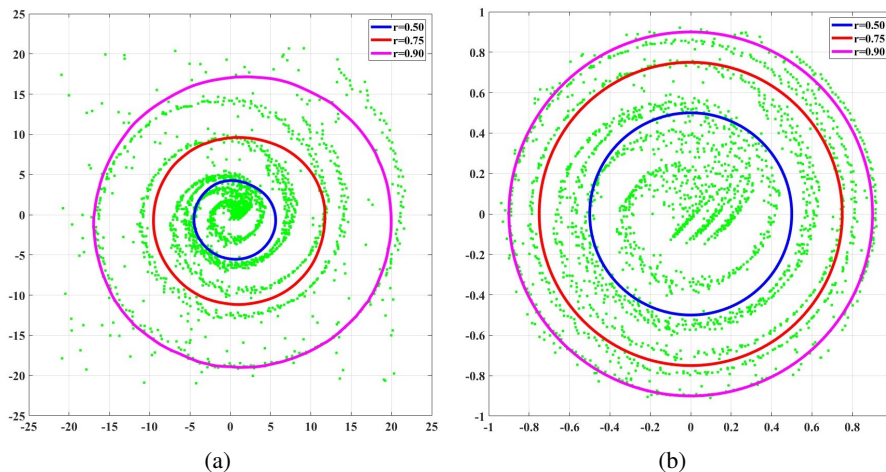


FIG 3. Spiral-shaped distribution with  $n = 2259$  sample points [48]. Figure 3(b) shows the K-transform and 3(a) shows the inverse K-transform. This example illustrates zoom-in effect and the low power of the K-transform method. Points in the empty spaces are within the  $r = 0.5$  M-quantile while points in the outer spiral of the data are outside the circle of radius 0.9 in the co-domain.

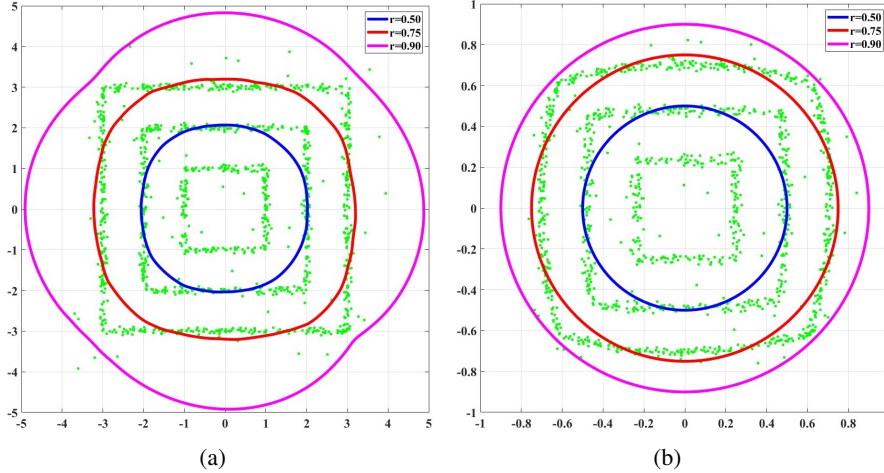


FIG 4. This example illustrates zoom-in effect and the low power of the K-transform method for a non-standard square-shaped distribution with  $n = 1242$  sample points [48]. Figure 4(b) shows the K-transform and 4(a) shows the inverse K-transform. Points in the empty spaces within the  $r = 0.5$  M-quantile should be outliers but are not classified as such by the method.

**5. Conclusion.** Regions of low probability density are commonly associated with outliers and anomalies in data. In this article, we have shown that for multivariate data on spaces with odd dimension  $d$  greater than or equal to three, it is not the K-transform  $\nabla f_\mu(s)$  that is directly proportional to the probability density, but the poly-Laplacian  $\Delta^{(d+1)/2} f_\mu(s)$  instead. This leads to the natural conclusion that the K-transform is not a useful object from which to attempt to compute “quantiles” in higher dimensions; a situation that is very different from the one-dimensional case. For the lowest even dimensional case of  $d = 2$ , we elucidate a zoom-in feature of the K-transform whereby regions of higher probability density are magnified when mapped to the co-domain. Due to this effect, it may not be appropriate to think of contours of equal radial distance from the origin in the co-domain as corresponding to quantiles. In summary, the established lore of interpreting the K-transform as a distribution and its inverse as a quantile function, applies only to the one-dimensional case.

#### APPENDIX A: ALGORITHM FOR COMPUTATION OF GEOMETRIC QUANTILES

In the following steps, we describe an MM type algorithm ([27]) for the computation of the geometric quantile in (6).

Step 0: Randomly choose an initial value of  $s$ , say  $s_0$ .

Step 1: Specify the surrogate objective function to be

$$(20) \quad \arg \min_{s \in \mathbb{R}^d} \frac{1}{2} \mathbb{E} \left( \frac{\|s - X\|_2^2}{\|s_0 - X\|_2} + \|s_0 - X\|_2 - 2\|X\|_2 \right) - \langle s, v \rangle, v \in B_1(0).$$

Step 2: Compute the gradient of (20) as,

$$(21) \quad v = \mathbb{E} \left( \frac{s - X}{\|s_0 - X\|_2} \right).$$

Step 3: For  $k \geq 1$ , iteratively update the value of  $s$  until convergence is reached.

$$(22) \quad s_k = \frac{v + \mathbb{E} (X \|s_{k-1} - X\|_2^{-1})}{\mathbb{E} (\|s_{k-1} - X\|_2^{-1})}.$$

## APPENDIX B: PROOF OF THEOREM 2.1

PROOF. Suppose  $dg(t)/dt$  and  $dh(t)/dt$  exist for all  $t \in (\alpha, \beta)$ , and let  $\{t + t_k\}_{k=1}^{\infty}$  be any sequence contained in  $(\alpha, \beta)$  converging to  $t$ . We then have:

$$\begin{aligned}
\frac{\phi(t + t_k) - \phi(t)}{t_k} &= \frac{1}{t_k} \left[ \int_{h(t+t_k)}^{g(t+t_k)} f(x, t + t_k) dx - \int_{h(t)}^{g(t)} f(x, t) dx \right] \\
&= \frac{1}{t_k} \left[ \int_{h(t+t_k)}^{g(t+t_k)} f(x, t + t_k) dx - \int_{h(t+t_k)}^{g(t)} f(x, t + t_k) dx \right] + \\
&\quad \frac{1}{t_k} \left[ \int_{h(t+t_k)}^{g(t)} f(x, t + t_k) dx - \int_{h(t)}^{g(t)} f(x, t + t_k) dx \right] + \\
&\quad \frac{1}{t_k} \left[ \int_{h(t)}^{g(t)} f(x, t + t_k) dx - \int_{h(t)}^{g(t)} f(x, t) dx \right] \\
(23) \quad &= \frac{1}{t_k} \left[ \int_{g(t)}^{g(t+t_k)} f(x, t + t_k) dx - \int_{h(t)}^{h(t+t_k)} f(x, t + t_k) dx \right] \\
&\quad + \frac{1}{t_k} \left[ \int_{h(t)}^{g(t)} [f(x, t + t_k) dx - f(x, t)] dx \right].
\end{aligned}$$

Let  $|f(t, x)| \leq M$  on  $[\alpha, \beta] \times [a, b]$  and  $|\partial f(t, x)/\partial t| \leq K$  on  $(\alpha, \beta) \times (a, b)$ . We note that for  $\varepsilon > 0$ , there exists  $\delta > 0$  such that for all  $|t_k| < \delta$  and  $x \in [a, b]$ ,  $|f(x, t + t_k) - f(x, t)| < K |t - t_k|$ . In addition, since  $g$  is Lipschitz continuous, we have that

$$\begin{aligned}
\left| \frac{1}{t_k} \int_{g(t)}^{g(t+t_k)} (f(x, t + t_k) - f(x, t)) dx \right| &\leq \left| \frac{1}{t_k} \int_{g(t)}^{g(t+t_k)} |f(x, t + t_k) - f(x, t)| dx \right| \\
&\leq \left| \frac{K}{t_k} \int_{g(t)}^{g(t+t_k)} |t + t_k - t| dx \right| \\
&\leq K |g(t + t_k) - g(t)| \\
&\leq K \|g\|_{\infty} |t_k|.
\end{aligned}$$

Therefore,

$$(24) \quad \lim_{t_k \rightarrow 0} \left| \frac{1}{t_k} \int_{g(t)}^{g(t+t_k)} [f(x, t + t_k) - f(x, t)] dx \right| = 0.$$

Now, by the change of variable formula (see e.g., [33, Sec. 38.3]):

$$(25) \quad \frac{1}{t_k} \int_{g(t)}^{g(t+t_k)} f(x, t) dx = \frac{1}{t_k} \int_t^{t+t_k} f(g(\tau), t) g'(\tau) d\tau.$$

As this integrand is integrable, we then have by the Lebesgue Differentiation Theorem that for almost every  $t \in [\alpha, \beta]$ ,

$$(26) \quad \lim_k \frac{1}{t_k} \int_t^{t+t_k} f(g(\tau), t) g'(\tau) d\tau = f(g(t), t) g'(t).$$

By (24) and (26),

$$\begin{aligned}
\lim_k \frac{1}{t_k} \int_{g(t)}^{g(t+t_k)} f(x, t+t_k) dx &= \lim_k \frac{1}{t_k} \int_{g(t)}^{g(t+t_k)} [f(x, t+t_k) - f(x, t)] dx \\
&\quad - \lim_k \frac{1}{t_k} \int_{g(t)}^{g(t+t_k)} f(x, t) dx \\
(27) \qquad \qquad \qquad &= f(g(t), t) g'(t).
\end{aligned}$$

By the same approach, the second integral in (23) can be shown to be for almost every  $t \in [\alpha, \beta]$

$$(28) \qquad \lim_k \frac{1}{t_k} \int_t^{t+t_k} f(h(\tau), t+t_k) h'(\tau) d\tau = f(h(t), t) h'(t).$$

Consider now the final term in (23). Let  $x \notin E_0$ . By the Mean Value Theorem applied to the interval  $[t, t+t_k]$  or  $[t+t_k, t]$ , depending on the sign of  $t_k$ , we then have that:

$$\left| \frac{f(x, t+t_k) dx - f(x, t)}{t_k} \right| = \left| \frac{\partial f}{\partial t}(\bar{t}, x) \right| \leq K,$$

for some  $\bar{t}$  in the segment joining  $t$  and  $t+t_k$ . Now, invoking the (Lebesgue) Dominated Convergence Theorem, we obtain:

$$\begin{aligned}
\lim_k \int_{h(t)}^{g(t)} \frac{f(x, t+t_k) dx - f(x, t)}{t_k} dx &= \int_{h(t)}^{g(t)} \lim_k \frac{f(x, t+t_k) dx - f(x, t)}{t_k} dx \\
(29) \qquad \qquad \qquad &= \int_{[h(t), g(t)] \setminus E_0} \frac{\partial f}{\partial t}(\bar{t}, x) dt.
\end{aligned}$$

Collecting (27) – (29), we obtain finally that for almost every  $t \in (\alpha, \beta)$ :

$$\begin{aligned}
\frac{d}{dt} \phi(t) &= \lim_k \frac{1}{t_k} \left[ \int_{h(t+t_k)}^{g(t+t_k)} f(x, t+t_k) dx - \int_{h(t)}^{g(t)} f(x, t) dx \right] \\
(30) \qquad \qquad &= f(t, g(t)) \frac{dg(t)}{dt} - f(t, h(t)) \frac{dh(t)}{dt} + \int_{[h(t), g(t)] \setminus E_0} \frac{\partial}{\partial t} f(t, x) dx.
\end{aligned}$$

□

### APPENDIX C: PROOF OF LEMMA 3.2

PROOF. Set  $z = x - s$ . Denote  $r = \|z\|$ . We will use the volume form for  $\mathbb{R}^d$  in the coordinates  $z$ .

$$\begin{aligned}
\int_{\mathbb{R}^d} \|s - x\|_2^{-k} \rho(x) dV(x) &= \int_{B_1(0)} \|z\|_2^{-k} \rho(z+s) dV(z) + \int_{B_1^c(0)} \|z\|_2^{-k} \rho(z+s) dV(z) \\
&= \int_{B_1(0)} \rho(z+s) r^{d-1-k} dr d\sigma_{d-1}(\Phi_{d-1}) + \int_{\mathbb{R}^d \setminus B_1(0)} \rho(z+s) r^{d-1-k} dr d\sigma_{d-1}(\Phi_{d-1}).
\end{aligned}$$

As  $k \geq 0$ ,

$$r^{d-1-k} \leq \begin{cases} 1; & r \leq 1 \\ r^{d-1}; & r > 1. \end{cases}$$

Hence,

$$\begin{aligned}
\int_{\mathbb{R}^d} \|s - x\|_2^{-k} \rho(x) dV(x) &\leq \int_{B_1(0)} \rho(z + s) dr d\sigma_{d-1}(\Phi_{d-1}) + \int_{\mathbb{R}^d \setminus B_1(0)} \rho(z + s) r^{d-1} dr d\sigma_{d-1}(\Phi_{d-1}) \\
&\leq \|\rho\|_\infty \int_{B_1(0)} dr d\sigma_{d-1}(\Phi_{d-1}) + \int_{\mathbb{R}^d} \rho(z + s) r^{d-1} dr d\sigma_{d-1}(\Phi_{d-1}) \\
&< C + 1 \\
&< \infty.
\end{aligned}$$

□

#### APPENDIX D: PROOF OF LEMMA 3.3

PROOF. Write  $\|\cdot\|$  to mean the usual Euclidean norm  $\|\cdot\|_2$  in order to simplify the notation in the rest of the proof. There is a need for subtlety because the integrands of  $G$  and its proposed gradient are undefined for  $x = s$ . We need to excise a small region around the point  $s$  in the variable  $x$  while dealing with the integrals. To this end, let  $R > 0$ . Since the integrand of  $G(s)$  given by  $g(s, x) = \|s - x\|^{-k}$  is a differentiable and bounded function on  $\mathbb{R}^d \setminus B_R(s)$ , then for  $h \in \mathbb{R}^d$  satisfying  $0 < \|h\| < R/2$ , we have by the Mean Value Theorem that for all  $x \in \mathbb{R}^d \setminus B_R(s)$ ,

$$(31) \quad g(s + h, x) - g(s, x) = \int_0^1 \nabla_s g(s + ch, x) dc \cdot h.$$

where for  $a, b \in \mathbb{R}^d$ ,  $a \cdot b = \langle a, b \rangle$  denotes the usual vector dot product. Hence,

$$\begin{aligned}
\frac{|g(s + h, x) - g(s, x) - \nabla_s g(s, x) \cdot h|}{\|h\|} &\leq \left\| \int_0^1 \nabla_s g(s + ch, x) dc \right\| + \|\nabla_s g(s, x)\| \\
&= \left\| -k \int_0^1 \frac{s + ch - x}{\|s + ch - x\|^{k+2}} dc \right\| + k \left\| \frac{s - x}{\|s - x\|^{k+2}} \right\| \\
&\leq k \int_0^1 \|s + ch - x\|^{-k-1} dc + k \|s - x\|^{-k-1}.
\end{aligned}$$

Integrating over  $\mathbb{R}^d \setminus B_R(s)$ , we obtain,

$$(32) \quad \int_{\mathbb{R}^d \setminus B_R(s)} \frac{|g(s + h, x) - g(s, x) - \nabla_s g(s, x) \cdot h|}{\|h\|} \rho(x) dV(x)$$

$$(33) \quad \leq \int_{\mathbb{R}^d \setminus B_R(s)} k \left( \int_0^1 \|s + ch - x\|^{-k-1} dc + \|s - x\|^{-k-1} \right) \rho(x) dV(x)$$

$$(34) \quad \leq \int_{\mathbb{R}^d} k \left( \int_0^1 \|s + ch - x\|^{-k-1} dc + \|s - x\|^{-k-1} \right) \rho(x) dV(x).$$

By Lemma 3.2, we have that for all  $c \in [0, 1]$ ,

$$\int_{\mathbb{R}^d} k \|s + ch - x\|^{-k-1} \rho(x) dV(x) < \infty.$$

Defining

$$\theta = \max_{c \in [0, 1]} \int_{\mathbb{R}^d} k \|s + ch - x\|^{-k-1} \rho(x) dV(x),$$

we see that  $\theta$  is a real value (the maximum of a continuous function on a compact interval is achieved at a point in the interval). Hence we obtain that:

$$\int_0^1 \int_{\mathbb{R}^d} k \left( \|s + ch - x\|^{-k-1} + \|s - x\|^{-k-1} \right) \rho(x) dV(x) dc \leq 2\theta.$$

Now, by (34) and Tonelli, note that

$$\int_{\mathbb{R}^d \setminus B_R(s)} \frac{|g(s+h, x) - g(s, x) - \nabla_s g(s, x) \cdot h|}{\|h\|} \rho(x) dV(x) \leq 2\theta.$$

By the Mean Value Theorem applied to (31), and for each  $s$ , we have the following pointwise convergence as  $h \rightarrow 0$ :

$$\lim_{\|h\| \rightarrow 0} \frac{|g(s+h, x) - g(s, x) - \nabla_s g(s, x) \cdot h|}{\|h\|} \leq \lim_{\|h\| \rightarrow 0} \|\nabla_s g(s+ch, x) - \nabla_s g(s, x)\| = 0.$$

Therefore, by the Dominated Convergence Theorem,

$$\lim_{h \rightarrow 0} \frac{1}{\|h\|} \int_{\mathbb{R}^d \setminus B_R(s)} (g(s+h, x) - g(s, x) - \nabla_s g(s, x) \cdot h) \rho(x) dV(x) = 0.$$

By the definition of the Frechet derivative, we have:

$$\begin{aligned} \nabla_s \int_{\mathbb{R}^d \setminus B_R(s)} g(s, x) \rho(x) dV(x) &= \int_{\mathbb{R}^d \setminus B_R(s)} \nabla_s g(s, x) \rho(x) dV(x) \\ &= -k \int_{\mathbb{R}^d \setminus B_R(s)} \frac{(s-x)}{\|s-x\|^{k+2}} \rho(x) dV(x). \end{aligned}$$

Noting that this result does not depend on  $R > 0$ , let  $R \rightarrow 0$  to obtain:

$$\lim_{R \rightarrow 0} \nabla_s \int_{\mathbb{R}^d \setminus B_R(s)} g(s, x) \rho(x) dV(x) = -k \lim_{R \rightarrow 0} \int_{\mathbb{R}^d \setminus B_R(s)} \frac{(s-x)}{\|s-x\|^{k+2}} \rho(x) dV(x).$$

Due to Lemma 3.2, the integral on the right hand side converges absolutely and uniformly as  $R \rightarrow 0$ , and for any  $0 \leq k \leq d-2$ . Due to the same lemma, the integral on the left hand side also converges for each  $s$  to  $\int_{\mathbb{R}^d} g(s, x) \rho(x) dV(x)$ . Therefore, by a standard result in analysis (e.g., Theorem 7.17 in [41]), the above integrals are equal over all of  $\mathbb{R}^d$ :

$$\nabla_s \int_{\mathbb{R}^d} g(s, x) \rho(x) dV(x) = -k \int_{\mathbb{R}^d} \frac{(s-x)}{\|s-x\|^{k+2}} \rho(x) dV(x).$$

□

(A simple modification of the proof also works for integrands the type  $\phi(g(s, x))$  where  $\phi$  is a differentiable function.)

#### APPENDIX E: PROOF OF LEMMA 3.4

PROOF. Once again write  $\|\cdot\|$  to mean the usual Euclidean norm  $\|\cdot\|_2$ . In Lemma 3.3, we showed that under the given conditions on  $\rho$ , the Frechet derivative of  $G$  with respect to  $s$  is given by,

$$(35) \quad \nabla_s G(s) = -k \int_{\mathbb{R}^d} \frac{s-x}{\|s-x\|^{k+2}} \rho(x) dV(x).$$

Below we repeat the steps of the proof of Lemma 3.4, which hold even in the presence of the additional complication that the integrand in (35) is a vector function of  $s$ . Let  $R > 0$

and  $g_1(s, x) = -k(s-x)\|s-x\|^{-(k+2)}$ , which is bounded and differentiable on  $\mathbb{R}^d \setminus B_R(s)$ . Now, for  $h \in \mathbb{R}^d$  satisfying  $0 < \|h\| < R/2$ , an application of the Mean Value Theorem yields that for all  $x \in \mathbb{R}^d \setminus B_R(s)$ ,

$$(36) \quad g_1(s+h, x) - g_1(s, x) = \left[ \int_0^1 D_s g_1(s+ch, x) dc \right] \cdot h$$

Noting that,

$$\begin{aligned} & \left\| \left[ -k \int_0^1 \left( \frac{I_d}{\|s+ch-x\|^{k+2}} - \frac{(k+2)(s+ch-x)(s+ch-x)^t}{\|s+ch-x\|^{k+4}} \right) dc \right] \cdot h \right\| \\ & \leq \int_0^1 k \left( \frac{\sqrt{d}}{\|s+ch-x\|^{k+2}} + (k+2) \frac{\|s+ch-x\|^2}{\|s+ch-x\|^{k+4}} \right) dc \\ & \leq k(\sqrt{d} + k + 2) \int_0^1 \|s+ch-x\|^{-k-2} dc. \end{aligned}$$

we obtain,

$$(37) \quad \frac{|g_1(s+h, x) - g_1(s, x) - D_s g_1(s, x) \cdot h|}{\|h\|} \leq k(\sqrt{d} + k + 2) \left[ \int_0^1 \|s+ch-x\|^{-k-2} dc + \|s-x\|^{-k-2} \right].$$

Integrating both sides of (37) over  $\mathbb{R}^d \setminus B_R(s)$  yields,

$$(38) \quad \begin{aligned} & \int_{\mathbb{R}^d \setminus B_R(s)} \frac{|g_1(s+h, x) - g_1(s, x) - D_s g_1(s, x) \cdot h|}{\|h\|} \rho(x) dV(x) \\ & \leq k(\sqrt{d} + k + 2) \int_{\mathbb{R}^d \setminus B_R(s)} \left[ \int_0^1 \|s+ch-x\|^{-k-2} dc + \|s-x\|^{-k-2} \right] \rho(x) dV(x) \\ & \leq k(\sqrt{d} + k + 2) \int_{\mathbb{R}^d} \left[ \int_0^1 \|s+ch-x\|^{-k-2} dc + \|s-x\|^{-k-2} \right] \rho(x) dV(x). \end{aligned}$$

By Lemma 3.3, we have that for all  $c \in [0, 1]$ ,

$$(39) \quad \int_{\mathbb{R}^d} k(\sqrt{d} + k + 2) \|s+ch-x\|^{-k-2} \rho(x) dV(x) < \infty.$$

Denoting

$$(40) \quad \nu = \max_{c \in [0, 1]} \int_{\mathbb{R}^d} k(\sqrt{d} + k + 2) \|s+ch-x\|^{-k-2} \rho(x) dV(x),$$

we have immediately that,

$$(41) \quad \int_0^1 \int_{\mathbb{R}^d} k(\sqrt{d} + k + 2) \left( \|s+ch-x\|^{-k-2} + \|s-x\|^{-k-2} \right) \rho(x) dV(x) dc \leq 2\nu.$$

Now, from (38) we have from Fubini's Theorem that,

$$(42) \quad \int_{\mathbb{R}^d \setminus B_R(s)} \frac{|g_1(s+h, x) - g_1(s, x) - D_s g_1(s, x) \cdot h|}{\|h\|} \rho(x) dV(x) \leq 2\nu.$$

By (36), for each  $s$ , the function  $(g_1(s+h, x) - g_1(s, x) - D_s g_1(s, x) \cdot h) / \|h\|$  converges pointwise to 0 as  $h \rightarrow 0$ , since

$$\begin{aligned} \lim_{\|h\| \rightarrow 0} \frac{|g_1(s+h, x) - g_1(s, x) - D_s g_1(s, x) \cdot h|}{\|h\|} &\leq \lim_{\|h\| \rightarrow 0} \left\| \int_0^1 D_s g_1(s + ch, x) dc - D_s g_1(s, x) \right\| \\ &= \left\| \int_0^1 D_s g_1(s, x) dc - D_s g_1(s, x) \right\| \\ &= 0, \end{aligned}$$

whence, by Lebesgue's Dominated Convergence Theorem,

$$(43) \quad \lim_{h \rightarrow 0} \int_{\mathbb{R}^d \setminus B_R(s)} \frac{|g_1(s+h, x) - g_1(s, x) - D_s g_1(s, x) \cdot h|}{\|h\|} \rho(x) dV(x) = 0.$$

By the definition of the Frechet derivative,

$$\begin{aligned} D_s \int_{\mathbb{R}^d \setminus B_R(s)} g_1(s, x) \rho(x) dV(x) &= \int_{\mathbb{R}^d \setminus B_R(s)} D_s g_1(s, x) \rho(x) dV(x) \\ &= -k \int_{\mathbb{R}^d \setminus B_R(s)} \left( \frac{I_d}{\|s-x\|^{k+2}} - (k+2) \frac{(s-x)(s-x)^t}{\|s-x\|^{k+4}} \right) \rho(x) dV(x). \end{aligned}$$

Finally, letting  $R \rightarrow 0$  yields the desired result by the same argument used at the end of Lemma 3.3.  $\square$

#### APPENDIX F: PROOF OF LEMMA 3.5

PROOF. For  $0 < \varepsilon < 1$ , there exists  $[t_1, t_2]$  such that  $\mu([t_1, t_2]) > 1 - \varepsilon$ . Let  $s \in [t_1, t_2]$  and  $\{s_k\}_{k=1}^\infty$  be a sequence converging to 0. Define,

$$(44) \quad f_\mu(s) = \int_{\mathbb{R}} (|s-x| - |x|) \rho(x) dx,$$

$$(45) \quad \phi(s; t_1, t_2) = \int_{[t_1, t_2]} (|s-x| - |x|) \rho(x) dx.$$

As  $\rho$  is a pdf, for each  $s$  the function  $\theta(x) := (|s-x| - |x|) \rho(x) \in L^1([t_1, t_2])$ . Therefore,

$$\frac{\phi(s+s_k; t_1, t_2) - \phi(s; t_1, t_2)}{s_k} = \frac{1}{s_k} \int_{[t_1, t_2]} (|s+s_k-x| - |s-x|) \rho(x) dx := A + B,$$

where

$$A = \frac{1}{s_k} \left[ \int_{t_1}^{s+s_k} (s+s_k-x) \rho(x) dx - \int_{t_1}^s (s-x) \rho(x) dx \right],$$

and

$$B = \frac{1}{s_k} \left[ \int_{s+s_k}^{t_2} (s+s_k-x) \rho(x) dx - \int_s^{t_2} (s-x) \rho(x) dx \right].$$

Now note that

$$\begin{aligned} A &= \frac{1}{s_k} \int_{t_1}^s s_k \rho(x) dx + \frac{1}{s_k} \int_s^{s+s_k} (s+s_k-x) \rho(x) dx \\ &= \mu([t_1, s]) + \frac{1}{s_k} \int_s^{s+s_k} (s+s_k-x) \rho(x) dx, \end{aligned}$$

and similarly,

$$B = -\mu([s, t_2]) + \frac{1}{s_k} \int_s^{s+s_k} (s + s_k - x) \rho(x) dx.$$

Putting things together,

$$\frac{\phi(s + s_k; t_1, t_2) - \phi(s; t_1, t_2)}{s_k} = \mu([t_1, s]) - \mu([s, t_2]) + \frac{2}{s_k} \int_s^{s+s_k} (s + s_k - x) \rho(x) dx.$$

By Theorem 2.1 applied to  $(s, y) \in [t_1, t_2] \times [t_1, t_2]$ , yields that, for almost all  $s \in [t_1, t_2]$ ,

$$(46) \quad \left. \frac{d}{dy} \right|_{y=s} \int_s^y (y - x) \rho(x) dx = 0 \implies \lim_{s_k \rightarrow 0} \frac{1}{s_k} \int_s^{s+s_k} (s + s_k - x) \rho(x) dx = 0.$$

It follows that for almost all  $s \in [t_1, t_2]$ ,

$$\phi'(s) = \mu([t_1, s]) - \mu([s, t_2]) = \mu([-\infty, s]) - \mu([s, \infty]) + 2\varepsilon.$$

Letting  $\varepsilon \rightarrow 0$ , we see that for almost all  $s \in \mathbb{R}$ ,  $f'_\mu(s) = \mu([-\infty, s]) - \mu([s, \infty])$ . Now, applying Leibnitz's rule (2nd fundamental theorem of calculus), yields that, for almost all  $s \in \mathbb{R}$ ,

$$(47) \quad f''_\mu(s) = \rho(s) - (-\rho(s)) = 2\rho(s),$$

thus proving the desired result. If  $\rho$  is a continuous function, then (the same Riemann integral version of) Leibnitz's rule may be employed in (46) instead of Theorem 2.1 to conclude (47) for all  $s \in \mathbb{R}$ .  $\square$

#### APPENDIX G: PROOF OF THEOREM 3.6

By Lemma 3.3, we can obtain the gradient of  $f_\mu(s)$  as,

$$(48) \quad \nabla_s f_\mu(s) = \mathbb{E} \left( \frac{s - X}{\|s - X\|_2} \right),$$

and by Lemma 3.4 we can compute its Hessian as

$$(49) \quad D_s \nabla_s f_\mu(s) = \mathbb{E} \left( \frac{I_d}{\|s - X\|_2} - \frac{(s - X)(s - X)^t}{\|s - X\|_2^3} \right),$$

which we note is symmetric and positive definite. Hence, we can compute the Laplacian of  $f_\mu$  as

$$(50) \quad \Delta_s f_\mu(s) = \text{trace}(D_s \nabla_s f_\mu(s)) = (d - 1) \mathbb{E} \left( \frac{1}{\|s - X\|_2} \right).$$

Now, by Lemma 3.2,  $\Delta_s f_\mu(s)$  exists for  $d \geq 3$ , so that (16) holds for  $j = 1$ . Proceeding by induction, we suppose that (16) holds for all  $j \in \{1, \dots, N - 1\}$ , and aim to show that (16) holds also for  $j + 1$ .

To this effect, set  $k = 2j - 1$ , and using Lemmas 3.2 and 3.4, we compute, respectively, the Frechet gradient and Hessian of  $\mathbb{E}\|s - X\|_2^{-k}$  as:

$$(51) \quad \nabla_s \mathbb{E} \left( \frac{1}{\|s - X\|_2^k} \right) = -k \mathbb{E} \left( \frac{s - X}{\|s - X\|_2^{k+2}} \right),$$

and

$$(52) \quad D_s \nabla_s \mathbb{E} \left( \frac{1}{\|s - X\|_2^k} \right) = -k \mathbb{E} \left( \frac{I_d}{\|s - X\|_2^{k+2}} - (k + 2) \frac{(s - X)(s - X)^t}{\|s - X\|_2^{k+4}} \right).$$

Hence, the Laplacian of  $\mathbb{E}\|s - X\|_2^{-k}$  is given by:

$$(53) \quad \Delta_s \mathbb{E} \left( \frac{1}{\|s - X\|_2^k} \right) = -k(d - k - 2) \mathbb{E} \left( \frac{1}{\|s - X\|_2^{k+2}} \right).$$

Now, the expectation on the right hand side of (53) exists by Lemma 3.3, as long as  $k \leq d - 2$ , or equivalently,  $j \leq N$ . Converting back to the  $j$  variable, as  $\Delta_s^j f_\mu(s) = \Delta_s (\Delta_s^{j-1} f_\mu(s))$ , yields the final result.

#### APPENDIX H: PROOF OF COROLLARY 1

PROOF. Consider the Poisson equation,

$$(54) \quad \Delta \phi(s) = \rho(s), \quad \text{a.e.},$$

whose fundamental solution is

$$\phi(s) = \frac{\Gamma(\frac{d}{2} + 1)}{d(d-2)\pi^{d/2}} \mathbb{E} \left( \frac{1}{\|s - X\|_2^{d-2}} \right).$$

Putting (18) and (54) together, we obtain:

$$\begin{aligned} \Delta^N f_\mu(s) &= (-1)^{N-1} (d-1) \cdots (2) \mathbb{E} \left( \frac{1}{\|s - X\|_2^{d-2}} \right) \\ &= (-1)^{N-1} (d-1) \cdots (2) d(d-2) \frac{\pi^{d/2}}{\Gamma(\frac{d}{2} + 1)} \phi(s), \end{aligned}$$

so that

$$\begin{aligned} \Delta \Delta^N f_\mu(s) &= (-1)^{N-1} (d-1) \cdots (2) \mathbb{E} \left( \frac{1}{\|s - X\|_2^{d-2}} \right) \\ &= (-1)^{N-1} (d-1) \cdots (2) d(d-2) \frac{\pi^{d/2}}{\Gamma(\frac{d}{2} + 1)} \rho(s), \quad \text{a.e.} \end{aligned}$$

thus proving the result.  $\square$

#### REFERENCES

- [1] AGGARWAL, C. (2015). *Data mining*. Springer.
- [2] ARYAL, G. (2016). Identifying a model of screening with multidimensional consumer heterogeneity. *Available at SSRN 2531188*.
- [3] BEN-GAL, I. (2005). Outlier detection. In *Data mining and knowledge discovery handbook* 131–146. Springer.
- [4] BRECKLING, J. and CHAMBERS, R. (1988). M-quantiles. *Biometrika* **75** 761–771.
- [5] BROWN, B. (1983). Statistical uses of the spatial median. *Journal of the Royal Statistical Society: Series B (Methodological)* **45** 25–30.
- [6] CHAKRABORTY, A. and CHAUDHURI, P. (2014). The spatial distribution in infinite dimensional spaces and related quantiles and depths. *The Annals of Statistics* **42** 1203–1231.
- [7] CHAKRABORTY, B. (2001). On affine equivariant multivariate quantiles. *Annals of the Institute of Statistical Mathematics* **53** 380–403.
- [8] CHAKRABORTY, B. and CHAUDHURI, P. (1996). On a transformation and re-transformation technique for constructing an affine equivariant multivariate median. *Proceedings of the American mathematical society* **124** 2539–2547.
- [9] CHANDOLA, V., BANERJEE, A. and KUMAR, V. (2009). Anomaly detection: a survey. *ACM computing surveys* **41** 15.

- [10] CHAOUCH, M. and GOGA, C. (2010). Design-based estimation for geometric quantiles with application to outlier detection. *Computational Statistics & Data Analysis* **54** 2214–2229.
- [11] CHAUDHURI, P. (1992). Multivariate location estimation using extension of R-estimates through U-statistics type approach. *The Annals of Statistics* **20** 897–916.
- [12] CHAUDHURI, P. (1996). On a geometric notion of quantiles for multivariate data. *Journal of the American statistical association* **91** 862–872.
- [13] CHEN, Y., DANG, X., PENG, H. and BART JR., H. (2008). Outlier detection with the kernelized spatial depth function. *IEEE Transactions on Pattern Analysis and Machine Intelligence* **31** 288–305.
- [14] CHERNOZHUKOV, V., GALICHON, A., HALLIN, M. and HENRY, M. (2017). Monge–Kantorovich depth, quantiles, ranks and signs. *The Annals of Statistics* **45** 223–256.
- [15] CHURCH, J. C., CHEN, Y. and RICE, S. V. (2008). A spatial median filter for noise removal in digital images. In *IEEE SoutheastCon 2008* 618–623. IEEE.
- [16] DHAR, S. S., CHAKRABORTY, B. and CHAUDHURI, P. (2014). Comparison of multivariate distributions using quantile–quantile plots and related tests. *Bernoulli* **20** 1484 – 1506.
- [17] FIELD, C. and GENTON, M. G. (2006). The multivariate g-and-h distribution. *Technometrics* **48** 104–111.
- [18] FRAIMAN, R. and PATEIRO-LÓPEZ, B. (2012). Quantiles for finite and infinite dimensional data. *Journal of Multivariate Analysis* **108** 1–14.
- [19] GHOSAL, P. and SEN, B. (2022). Multivariate ranks and quantiles using optimal transport: Consistency, rates and nonparametric testing. *The Annals of Statistics* **50** 1012–1037.
- [20] GIRARD, S. and STUPFLER, G. (2017). Intriguing properties of extreme geometric quantiles. *REVSTAT-Statistical Journal* **15** 107–139.
- [21] HA, J., SEOK, S. and LEE, J.-S. (2015). A precise ranking method for outlier detection. *Information Sciences* **324** 88–107.
- [22] HALDANE, J. (1948). Note on the median of a multivariate distribution. *Biometrika* **35** 414–417.
- [23] HALLIN, M., DEL BARRIO, E., CUESTA-ALBERTOS, J. and MATRÁN, C. (2021). Distribution and quantile functions, ranks and signs in dimension  $d$ : A measure transportation approach. *The Annals of Statistics* **49** 1139–1165.
- [24] HERRMANN, K., HOFERT, M. and MAILHOT, M. (2018). Multivariate geometric expectiles. *Scandinavian Actuarial Journal* **2018** 629–659.
- [25] KOLTCHINSKII, V. I. (1997). M-estimation, convexity and quantiles. *The Annals of Statistics* **25** 435–477.
- [26] KONG, L. and MIZERA, I. (2012). Quantile tomography: using quantiles with multivariate data. *Statistica Sinica* 1589–1610.
- [27] LANGE, K. (2016). *MM optimization algorithms*. SIAM, Philadelphia, PA.
- [28] LI, J. (2018). EDF goodness-of-fit tests based on centre-outward ordering. *Journal of Nonparametric Statistics* **30** 973–989.
- [29] LI, J., ZHANG, X. and JESKE, D. R. (2013). Nonparametric multivariate CUSUM control charts for location and scale changes. *Journal of Nonparametric Statistics* **25** 1–20.
- [30] LOPUHAA, H. and ROUSEEUW, P. (1991). Breakdown points of affine equivariant estimators of multivariate location and covariance matrices. *The Annals of Statistics* **19** 229–248.
- [31] MARDEN, J. I. (2004). Positions and QQ plots. *Statistical Science* 606–614.
- [32] MCCANN, R. J. (2001). Existence and uniqueness of monotone measure-preserving maps. *Duke Mathematical Journal* **80** 309–323.
- [33] MCSHANE, E. J. and BOTTS, T. A. (2005). *Real Analysis*. Dover reprinted from 1959.
- [34] MOSLER, K. (2013). *Depth Statistics In Robustness and Complex Data Structures: Festschrift in Honour of Ursula Gather* 17–34. Springer, Berlin, Heidelberg.
- [35] MUKHOPADHYAY, N. D. and CHATTERJEE, S. (2011). High dimensional data analysis using multivariate generalized spatial quantiles. *Journal of multivariate analysis* **102** 768–780.
- [36] OJA, H. (1983). Descriptive statistics for multivariate distributions. *Statistics & Probability Letters* **1** 327–332.
- [37] OJA, H. (2013). *Multivariate Median In Robustness and Complex Data Structures: Festschrift in Honour of Ursula Gather* 3–15. Springer, Berlin, Heidelberg.
- [38] PURI, M. L. and SEN, P. K. (1971). *Nonparametric methods in multivariate analysis*. John Wiley & sons.
- [39] RIZZI, A., VICHI, M. and BOCK, H. H. (1998). Multivariate  $L^1$  median. In *Proc. 6th conf. of the International Federation of Classification Societies* 539–546.
- [40] ROCKAFELLAR, R. T. (1970). *Convex analysis* **18**. Princeton university press.
- [41] RUDIN, W. (1976). *Principles of mathematical analysis*, 3 ed. McGraw Hill International.
- [42] SERFLING, R. (2002). Quantile functions for multivariate analysis: approaches and applications. *Statistica Neerlandica* **56** 214–232.
- [43] SERFLING, R. (2002). A depth function and a scale curve based on spatial quantiles. In *Statistical data analysis based on the  $L_1$ -norm and related methods* 25–38. Springer.

- [44] SMALL, C. G. (1990). A survey of multidimensional medians. *International Statistical Review* **58** 263-277.
- [45] STROOCK, D. (2011). *Probability Theory: an analytic view*. Cambridge University Press.
- [46] TARABELLONI, N., SCHENONE, E., COLLIN, A., IEVA, F., PAGANONI, A. M., GERBEAU, J.-F. et al. (2018). Statistical assessment and calibration of numerical ecg models. *JP Journal of Biostatistics* **15** 151–173.
- [47] TUKEY, J. W. (1977). *Exploratory data analysis*. Addison-Wesley Publishing Company.
- [48] XIE, J., XIONG, Z., DAI, Q., WANG, X. and ZHANG, Y. (2020). A local-gravitation-based method for the detection of outliers and boundary points. *Knowledge-Based Systems* **192** 105331.
- [49] ZUO, Y. and SERFLING, R. (2000). General notions of statistical depth function. *The Annals of statistics* 461–482.